Fluorescence spectroscopy and multivariate analysis as a greener monitoring tool: characterization of the curing kinetics of bioinspired polymers

Julieta Ledesma, Santiago A. Bortolato, Débora M. Martino & Carlos E. Boschetti

Published online: 12 Sep 2015.

Submit your article to this journal ⤷

View related articles ⤷

View Crossmark data ⤷

Taylor & Francis
Taylor & Francis Group

RESEARCH LETTER

Fluorescence spectroscopy and multivariate analysis as a greener monitoring tool: characterization of the curing kinetics of bioinspired polymers

Julieta Ledesma[a], Santiago A. Bortolato[b], Débora M. Martino[c] and Carlos E. Boschetti[a*]

[a]*Área Tecnología Química, Facultad de Ciencias Bioquímicas y Farmacéuticas, Universidad Nacional de Rosario, Instituto de Procesos Biotecnológicos y Químicos (IPROBYQ, CONICET-UNR), Suipacha 531 (S2002LRK) Rosario, Argentina;* [b]*Instituto de Química de Rosario (IQUIR, CONICET-UNR), Suipacha 570 (S2002LRK) Rosario, Argentina;* [c]*Instituto de Física del Litoral (IFIS Litoral, CONICET-UNL), Güemes 3450 (S3000GLN) Santa Fe, Argentina*

The photo-induced curing kinetics of bioinspired copolymers vinylbenzyl thymine (VBT) and vinylphenyl sulfonate was studied using fluorescence spectroscopy in combination with multivariate analysis. Fluorescence spectroscopy enables a detailed description of the curing process of VBT copolymers in real time, combining selectivity, simplicity and sensitivity, without the need of sample pre-treatments, being an advantage from the green analytical chemistry point of view. Two chemometric strategies were used to decompose the data matrix generated while monitoring the curing reaction, identifying the evolution of each species involved in the process in conjunction with the corresponding pure spectra. A comprehensive comparison between the developed approaches was made, clearly highlighting the advantages and disadvantages of both of them. The use of multivariate analysis applied to fluorescence spectroscopic data to study curing reactions have several advantages such as no sample pre-treatment, no sophisticated equipment requirement, reduced analysis time and use of non-toxic solvents, among others.

Keywords: Biopolymers; thymine; photo-induced curing kinetics; multivariate analysis; fluorescence spectroscopy

1. Introduction

Over the last century, a huge amount of synthetic polymers have been incorporated and have transformed our daily lives. However, the distinctiveness of durability and strength that make them useful also ensure their persistence in the environment and preclude their degradation. Nature constantly fabricates materials according to certain designs and strategies, which are taken as inspiration for Green Chemistry development. In order to develop new environmentally benign materials, different natural mechanisms have been inspected, identifying processes potentially adaptable to synthetic systems. For example, it is known that adjacent thymine bases at different positions of the DNA may suffer a dimerization reaction in presence of ultraviolet light (UV, $\lambda \sim 280$ nm) (*1*). This photochemical property of thymine moieties, which is harmful to the DNA, can be used to design polymeric materials in which the photo-induced cross-linking is advantageous. A novel monomer vinylbenzyl thymine (VBT) was synthesized by bioinspiration having the ability to photodimerize (*2*). Moreover, water-soluble polymers can be produced by copolymerizing VBT with ionic monomers

as vinylphenyl sulfonate (VPS) or vinylbenzyl triethylammonium chloride (VBA) (*3–6*). The copolymers coated on a solid substrate and irradiated with low UV doses undergo a dimerization reaction (curing reaction) between adjacent thymine, achieving an attractive functionalized copolymer of technological relevance (*7–10*). Despite the increasing technological applications, the basic characterization of the physical–chemical properties of the biopolymers is an emerging field of research.

It has been shown that UV–Vis and FTIR spectroscopies are useful tools for monitoring the curing reaction of VBT copolymers. Barbarini and co-workers demonstrated using UV–Vis spectroscopy that, for VBT-VBA copolymers of different compositions, the kinetics of the cross-linking reaction pointed to be a second-order process with respect to the thymine concentration (*11*). However, the complexity of the spectroscopic signals due to the presence of spurious species or impurities not relevant for the curing process prevents the acquisition of accurate information of interest. In recent years, the improvement of mathematical data treatments allowed the development of solvent-free methodologies based on direct

*Corresponding author. Email: cboschet@fbioyf.unr.edu.ar

measurements on solid samples without any sample chemical pre-treatment (*12–13*), which are able to mathematically differentiate the signals related to the species of interest. One such methodologies is multivariate curve resolution assisted by alternate least squares (MCR-ALS), that is currently a well-established chemometric model (*14*).

In particular, Garrido and co-workers presented a comprehensive review of the MCR-ALS capabilities to explain different chemical reactions (*15*). In addition, our experience in using MCR-ALS algorithm afforded improved results compared to previous findings (*11*) for the curing reaction of VBT copolymers in solid phase using first-order FTIR spectroscopy (*16*). However, the obtained results were only qualitative, given that the analytical signals were non-selective. According to IUPAC, selectivity is the extent to which a method can be used to determine particular analytes in mixtures or matrices without interferences from other elements of similar behavior (*17*). Therefore, it is an essential parameter to establish the efficacy of a proposed method for monitoring and quantification of compounds in varied samples.

Recently, Bortolato and co-workers (*18*) defined comprehensively the chemical reaction mechanism of the curing process of VBT-VBA copolymers, describing the underlying process in terms of identifiable steps, associated key parameters and equilibrium rate constants that characterize the interconversion and stability of diverse species involved by a second-order FTIR strategy. Additionally, the authors accomplished the quantification of all species, even in the presence of an interferent compound (*18*). FT-IR absorption spectra for different irradiation doses and different VBT-VBA copolymer compositions in solid phase were taken using grazing-angle specular-reflectance FT-IR spectroscopy, and the matrices were processed with MCR-ALS algorithm. Despite the high-quality results achieved, the developed method has significant drawbacks, which make it unattractive from an analytical point of view. The method has a low sensitivity, requiring a large amount of sample for a measurable outcome, uses expensive gold solid support, takes up extended time per sample and requires extreme care in sample handling. Therefore, from the perspective of green analytical chemistry, a new procedure that agrees in harmonious approach with this new paradigm needs to be developed (*19*).

Thymine has a well-known characteristic fluorescence spectrum (*20*). On the other hand, fluorescence spectroscopy enables a detailed description of unknown structures combining selectivity, simplicity and sensitivity. Fluorescence spectroscopy allows the study of the curing process of VBT copolymers in real time, without the need of sample pre-treatments. The present work reports the study of the curing kinetics of VBT and VPS copolymers of different monomer ratios coated on polyethylenterephthalate (PET) support by means of fluorescence spectroscopy. The chosen solid support has advantages and disadvantages. While PET is the support used in many papers to study the behavior of similar copolymers (*3, 11, 21*), it has been reported to have fluorescent signals in the same spectral regions of thymine (*22–24*). Therefore, the spectral selectivity of this technique may not be enough, and the accurate characterization of the species involved in the curing process could not be achieved. This drawback can be overcome by combining the fluorescence spectroscopic technique with MCR-ALS. To be able to apply MCR-ALS, the data must have a bilinear structure, meaning that the experimental data matrix (matrix of fluorescence intensities) must be expressed as product of a concentration matrix by a matrix containing the raw signal of the existing species (*25*). This condition is fulfilled by most spectroscopic techniques; consequently, by decomposing the data matrix generated while monitoring the cross-linking reaction, it is possible to identify the evolution of each species that occur in the process in concert with the corresponding pure spectra. As an advantage, the model makes possible to find information about the evolution of each species without previously understanding the reaction mechanism or establishing a kinetic model (*26*).

In this work, the photo-induced cross-linking kinetics of VBT-VPS copolymers was established by combining fluorescence spectroscopy and MCR-ALS chemometric models. For this purpose, copolymers of different VBT-VPS compositions were irradiated at 254 nm for different times and the emission and excitation fluorescence spectra were recorded. The information was used to determine the species involved in the curing process along with their relative or absolute concentrations and spectra, as well as the kinetic constants of the chemical reactions, via two different data-processing strategies. In addition, a comprehensive comparison between the developed MCR-ALS approaches was made, clearly highlighting the advantages and disadvantages of both of them. As a final point, to the best of our knowledge, the use of MCR-ALS applied to fluorescence spectroscopic data to study curing reactions of bioinspired polymers has not been reported before.

2. Theory

The main purpose in the analysis of an empirical chemical system is searching out useful information from raw experimental data and identifying the number of chemical components present in the

scrutinized portion. MCR-ALS (in three, four or *n*-ways) provides a linear model of individual component contributions through the raw experimental measurements, decomposing mathematically the raveled response from instrumental data into pure contributions due to each component in the system (*14, 25, 26*). The matrix structure of the MCR-ALS model is always the same, independently of the number of ways or modes that the considered data have. However, increasing the number of modes allows the access to more information, given that for non-selective systems this strategy may increase the selectivity of the species, at least in mathematical sense (*26*). Unlike other algorithms, with MCR-ALS model, there is no need of previous knowledge of chemical or physical expressions to analyze the data set (*25*). However, initial information obtained from the instrumental analysis has a positive influence on the resolution of the system, and can be used to build good initial estimates of concentration profiles and responses, as will be discussed later.

MCR-ALS transform the data matrix $\mathbf{D}$ into the dot product of two data matrices ($\mathbf{C}$ and $\mathbf{S}^T$) associated with the row (R) and the column (C) direction of $\mathbf{D}$, respectively. Each of them includes the pure response profiles of the N chemical compounds. In matrix notation, the general expression for this model is

$$\mathbf{D} = \mathbf{C} \cdot \mathbf{S}^T + \mathbf{E}, \qquad (1)$$

where $\mathbf{D}$ ($R \times C$) is the original data matrix, $\mathbf{C}$ ($R \times N$) and $\mathbf{S}^T$ ($N \times C$) are the matrices containing pure response profiles related to the data variation in the row and column directions, respectively; and $\mathbf{E}$ is the residual variation of the data set that is not related to any chemical contribution. When the $\mathbf{D}$ matrix is generated from several samples, it is commonly known in MCR-ALS paradigm as 'augmented' data matrix, since such matrix is built by placing all individual sample matrices adjacent to, or on top of, each other.

The employed chemometric strategies established the meaning of the indexes R and C. For a three-way approach and in terms of the data used in the present work, R contains the excitation-time merged profiles (augmented profile, in MCR-ALS terminology) of the N species involved in all the experiments, and C represents the emission spectra related to the N species. In the analyzed cases, the matrix $\mathbf{D}$ had the following dimensions for each three-way array (i.e. a single VBT-VPS composition): JL rows (J irradiation times, L excitation wavelengths) $\times$ K columns (K emission wavelengths), as shown in Figure 1.

Less clear is the meaning of the model matrices in the four-way data context. To implement MCR-ALS, it is mandatory to 'unfold' the original third-order data into matrices, and then be arranged into a linear 'super-augmented' matrix (*27*). Excitation-emission fluorescence matrices (EEFMs) of different VBT-VPS ratios measured at various irradiation times represent an original example of four-way data, in which the data modes are the irradiation times, the excitation and emission spectra, and the sample compositions.

The procedure used in the present work was different from that reported in relevant literature, given that most of the published works use data obtained from chromatographic techniques (*28–29*). In our case, VBT:VPS$_m$ samples of different composition (with $m = 1, 4, 8, 16$ or 32) were irradiated and an EEFM matrix ($L \times K$) was obtained, in which L and K are the number of excitation and emission wavelengths, respectively. This procedure was repeated from 0 to 180 min every 5 min, achieving a total of 37 times (J). Once the 37 EEFMs were obtained for each sample, the data were organized for the subsequent MCR-ALS analysis. In the first stage, each EEFM was unfolded, generating a row vector of dimensions ($1 \times LK$). Then, a ($J \times LK$) size matrix was created for each sample, and a super-augmented data matrix $\mathbf{D}$ of size ($JI \times LK$) was built, being I the number of samples under analysis. It is important to note that we have given proper meaning to the R (or JI) and C (or LK) indexes of Equation (1) in the four-way context.

After building the super-augmented matrix, and according to Equation (1), MCR-ALS analysis generates an augmented concentration matrix containing the pure irradiation time profiles for different samples ($\mathbf{C}$) in all JI fractions for the N-resolved components, a matrix of pure unfolded EEFM profiles ($\mathbf{S}^T$) for the N components, and a residual matrix ($\mathbf{E}$) containing noise and unresolved background. The single pure unfolded EEFM matrix $\mathbf{S}^T$ ($N \times LK$) can be reshaped into N different EEFMs (size $L \times K$, one for each component) and used for identification of the resolved components. On the other hand, the areas under the resolved irradiation time profiles corresponding to each sample ('scores') are used for quantitative purposes. In consequence, a matrix ($J \times N$) for every sample is obtained and, the concentration information included in $\mathbf{C}$ is used to build the univariate graph by plotting the compound concentration scores in function of the nominal component concentrations. Thus, the component concentration score can be defined for the ith sample by

$$a(i, n) = \sum_{j=1+(1-1)j} c(j, n), \qquad (2)$$
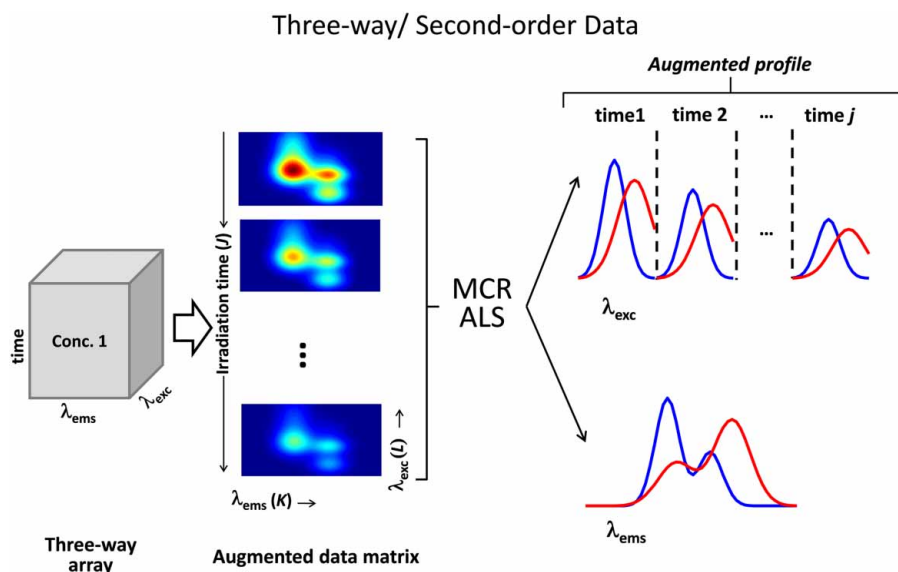
Three-way/ Second-order Data

Figure 1. Three-way (second-order) MCR-ALS.
Note: The meaning of indexes is explained in the text.

where $a(i,n)$ is the score for the component n in the sample i.

Figure 2 pictorially presents the entire procedure used to analyze four-way data with MCR-ALS.

Regardless of the number of ways of the processed data, the decomposition of matrix **D** is done throughout an iterative minimization procedure by alternating least squares of the Frobenius norm of **E**. To achieve good convergence, it is advantageous to initialize MCR-ALS with parameters as close as possible to the final results. Thus, spectra of the species are required since the resolution is based on the selectivity
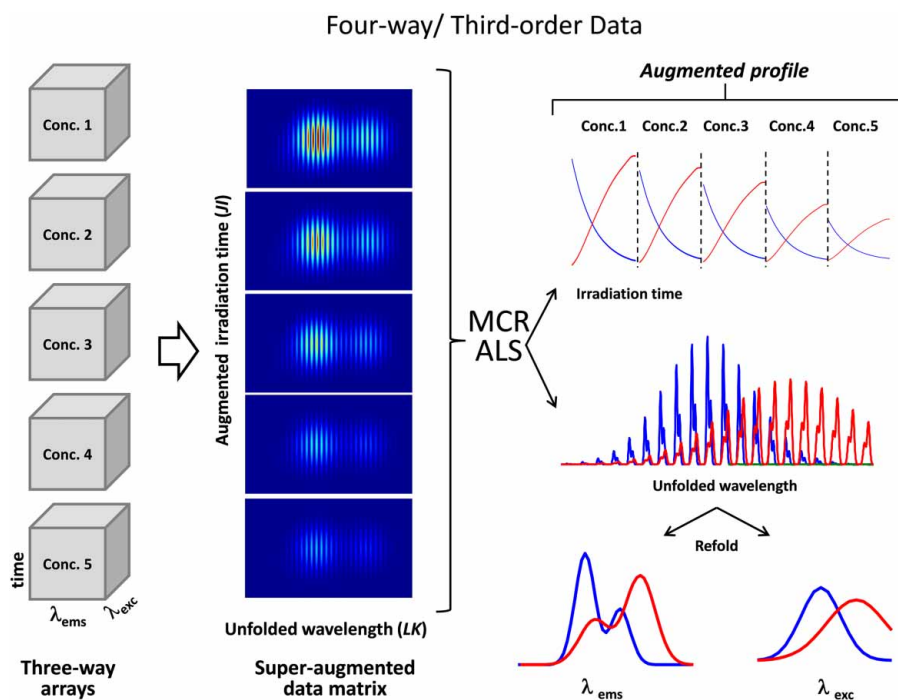
Four-way/ Third-order Data

Figure 2. Four-way (third-order) MCR-ALS.
Note: The meaning of indexes is explained in the text.

in the spectral mode, and it can be done by selecting the purest spectra for all the components, according to the SIMPLe-to-use Interactive Self-modeling Mixture Analysis algorithm (*30*). Several restrictions are also necessary to be imposed during the alternating least-squares fitting. In our case, the goal is to retrieve physically recognizable component profiles; therefore, non-negativity restrictions in concentrations and spectra are highly useful, letting the fitting to converge to a minimum with physical meaning.

Finally, to evaluate the performance of both MCR-ALS models used (three or four-ways), a comparison was made between the selectivity values (SEL) found by the algorithm in both cases. Clearly, the definition of selectivity discussed in the introduction must fit the multivariate scenario developed in this section. In that sense, several requirements have been proposed for a consistent numerical selectivity in MCR-ALS, being possible to define the following expression (*31*):

$$ \text{SEL} = \left[(\mathbf{S}^T\mathbf{S})^{-1} n \cdot n \right]^{-1/2}, \qquad (3) $$

where the element (*n,n*) indicates the analyte of interest, $\mathbf{S}^T$ contains the profiles of all sample components in the non-augmented direction (i.e. the emission spectra in the three-way mode, or the unfolded excitation-emission spectra in the four-way mode) and the superscript '–1' means matrix inversion.

3. Experimental work

3.1. Materials

All reagents were purchased in the purest available form and were used as received. Sodium hydroxide, isopropanol and acetone were purchased from Cicarelli (Buenos Aires, Argentina). Thymine, 4-vinylbenzyl chloride, 2,2'-azobis-2-methylpropionitrile (AIBN) and 2,6-di-tert-butyl-4-methylphenol were purchased from Sigma-Aldrich (Buenos Aires, Argentina). VBT was synthesized from thymine and vinylbenzyl chloride as described previously (*2*). VPS salt was purchased from Fluka (Buenos Aires, Argentina). Based on ^{1}H NMR spectra (Bruker 300 MHz NMR spectrometer), the monomeric products were deemed pure enough for the synthesis of the polymers.

Hydrophilic polyethylenterephthalate film (PET-X4C1, Dupont, USA) was used as substrate without previous treatment. Coatings were done using wire-round milled coating rods purchased from RDS Corp. (Webster, NY, USA). Irradiations were performed using a UV hand lamp (Spectroline ENF 260C, Spectronics Corporation Westbury, NY, USA).

3.2. Copolymer synthesis and characterization

To produce water-soluble co-polymers, VBT was copolymerized in a free radical process with the anionic monomer, VPS. The ratio of VBT:VPS monomers influences the behavior of the VBT polymeric system, and varies depending on the application. Therefore, $VBT_n:VPS_m$ have been synthesized with $n = 1$ and $m = 1, 4, 8, 16, 32$.

VBT:VPS 1:1 copolymer. To a 300 mL, 3-neck, round-bottom flask containing 250 mL of water/isopropanol (50:50) was added VBT (11.9 g, 0.049 mol) and VPS (10.1 g, 0.049 mol). The solution was heated to 65°C while stirring and 0.22 g of AIBN was added. Stirring was held for 18 h while the temperature was maintained at 65°C. The reaction mixture was cooled to room temperature and rotary evaporated to a concentration of 50%. By adding the aqueous solution to 1 L of cold acetone, the polymer was precipitated. Subsequently, the white solid precipitate was filtered and dried under vacuum. To verify the absence of unreacted monomers, the precipitated polymer was analyzed by ^{1}H NMR spectroscopy and the typical vinyl group signal at chemical shifts between 5 and 6 ppm was not observed in the spectra. Additionally, elemental analysis was used to confirm copolymer ratios (*18*).

VBT:VPS 1:4, 1:8, 1:16 and 1:32 copolymers. Identical procedures varying only the corresponding ratios of starting monomers were followed.

3.3. Copolymer curing: coating preparation, film irradiation and development

Aqueous solutions (10% w/w) of $VBT:VPS_m$ copolymers, with $m = 1, 4, 8, 16$ and 32, were prepared and homogenized by manual stirring. PET film was used as substrate without previous treatment. A known amount of aqueous copolymer solution was distributed homogeneously using a #06 wire-round milled coating rod, which resulted in coatings with wet thickness of 13.6 μm (*32*). The films were dried at room temperature for one hour, and then the copolymer-coated films were irradiated with a UV hand lamp at 254 nm and intensity of 1.3×10^{-3} W/cm², at different times (from 0 to 180 min, every 5 min). This process leads to the immobilization of the polymer in response to UV irradiation. The curing reaction was performed at room temperature, and as a consequence these coatings can be prepared on heat-sensitive materials. Finally, the cross-linking was monitored by solid-phase EEFMs as a function of irradiation time (equivalent to given energy).
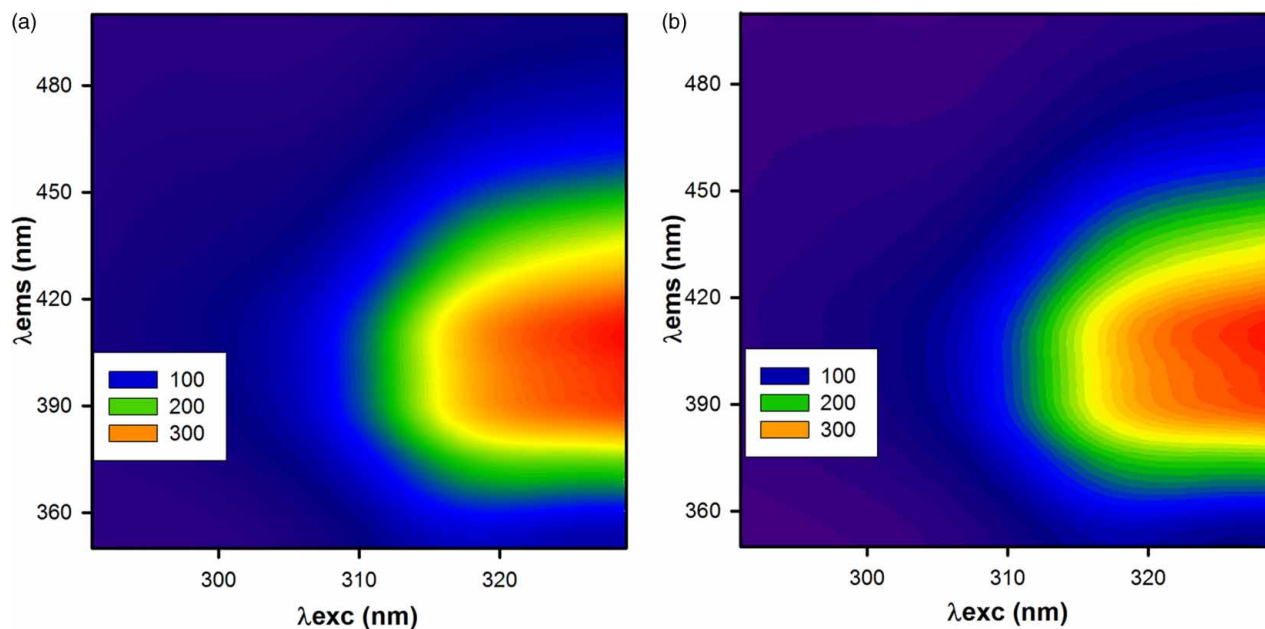
Figure 3. EEFMs of VBT:VPS$_1$ copolymer coatings for different irradiation times: (a) 0 min and (b) 180 min.

3.4. *Apparatus and software*

Solid-phase EEFMs measurements were taken using an excitation-emission Perkin-Elmer LS-55 luminescence spectrometer (Waltham, MA, USA) equipped with a xenon flash lamp. Excitation and emission slit widths were 10 nm, while the photomultiplier sensitivity was set on 700 V. The spectra were saved in ASCII format and transferred to a PC for subsequent manipulation. EEFMs were registered in the following conditions: λ_{exc} = 290–330 nm and λ_{ems} = 350–530 nm every 1 nm, irradiation between 0 and 180 min every 5 min, acquiring for each sample 37 EEFMs. The configuration used for the measurements involved the use of a PET film containing the sample, which was introduced into a usual quartz cell. In this way, the angle formed between the excitation and emission beams was 90°, with an incident angle of 45°.

The routines used for MCR-ALS were performed in MATLAB 7.0® (*33*) and are freely available on the Internet (http://www.ub.es/gesq/mcr/mcr.htm).

3.5. *MCR-ALS implementation*

In both approaches, three- and four-ways MCR-ALS, the number of components (five for all cases) was estimated by singular value decomposition, as explained in the Theory section. The initial assessments of the compound spectra were selected, taking into account the purest spectra for all the components, according to ref (*30*). Finally, in order to find physical meaningful solutions, the algorithm was set with the non-

negativity constraint in all data mode during the ALS optimization.

4. Results and discussion

Figure 3 shows two EEFMs corresponding to a VBT:VPS$_1$ copolymer without irradiation (Figure 3(a)), and a VBT:VPS$_1$ copolymer after 180 min of irradiation (Figure 3(b)). Interestingly, at first glance, few differences in the measured signal are observed, and such behavior is also evident for the other copolymer compositions (not shown). Thymine has a fluorescence emission maximum at 410 nm when the excitation wavelength range is set between 290–340 nm (*20*); therefore it is likely that the observed signal corresponds to thymine groups in VBT copolymers. However, as irradiation time increases, thymine moieties get cross-linked to generate the cyclobutane ring (*16, 18*). This effect cannot be easily observed on the EEFMs at different irradiation times, since only a mild reduction in the signal intensity can be seen, with no substantial changes of the spectra. In addition, it has been reported that the PET has a strong fluorescence in the evaluated regions, indicating that most of the observed signal belong to PET contribution. (*22, 23*) In summary, according to the presented evidence, the analyzed systems are highly complicated, justifying the use of chemometric strategies of different nature.

A three-way chemometric analysis of different samples was conducted in order to establish the

kinetic that govern the curing process. For each sample, an augmented **D** matrix of size 1480 (37 irradiation times, 40 excitation wavelengths) × 180 (emission wavelengths) was generated. The non-negativity constraint in all data mode was applied during the ALS optimization to find physical meaningful solutions. The amount of compounds (five for all samples) was estimated by singular value decomposition, and used to build the initial estimations (*14*). The purest spectra of the compounds were selected according to what was indicated in the Theory Section. Based on preliminary results, it was possible to postulate three species clearly present in the curing reaction (VBT, intermediate, final product), plus two species interfering on the measured signal but not influenced by the irradiation time (PET solid support and VPS monomer). The identification of the proposed interferents (PET and VPS) is supported by

two facts: first, the known fluorescence emission and excitation spectra of PET match the profiles given by the model, and, second, the amount of VPS present in each sample is proportional to the remaining signal obtained. This is also supported by the calculated similarity coefficient between the experimental spectra and the spectra recovered by the model (*26*), being 0.93 and 0.92 for PET emission and excitation spectrum, respectively. Figure 4 shows the algorithm outputs for copolymers of the largest and smallest percentage of VBT.

The information collected from the augmented excitation-time profile allows the characterization of the kinetics profiles corresponding to the species involved in the curing reaction for each sample (Figure 4(a)–(c)). The VBT excitation spectrum clearly gets smaller when increasing the irradiation time, as the excitation spectrum of the intermediate
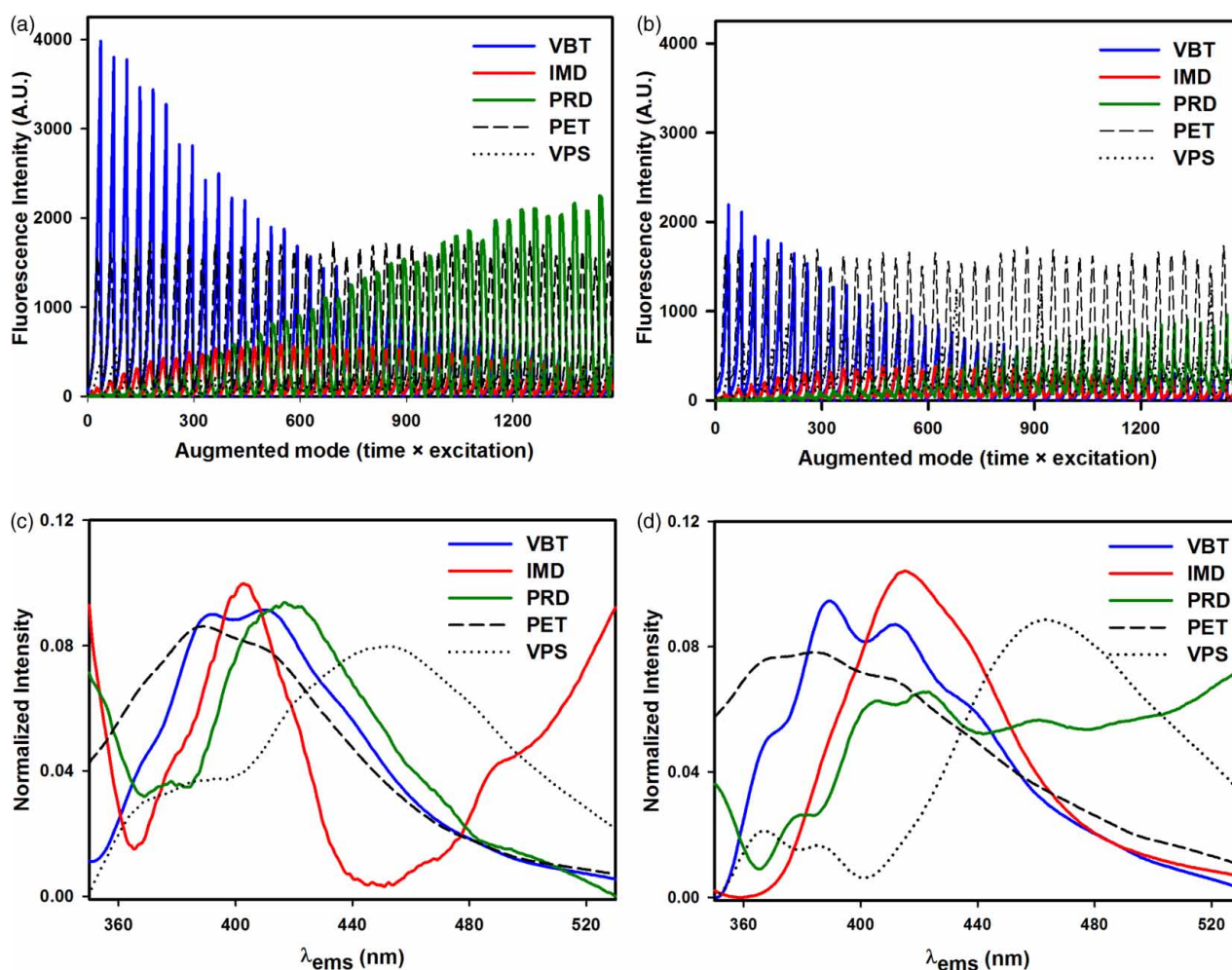

Figure 4. Outputs for the three-way MCR-ALS model. Augmented mode giving information on the curing reaction kinetics for (a) VBT:VPS$_1$ and (c) VBT:VPS$_{32}$; and emission spectral mode providing qualitative information of the sample components for (b) VBT:VPS$_1$ and (d) VBT:VPS$_{32}$.
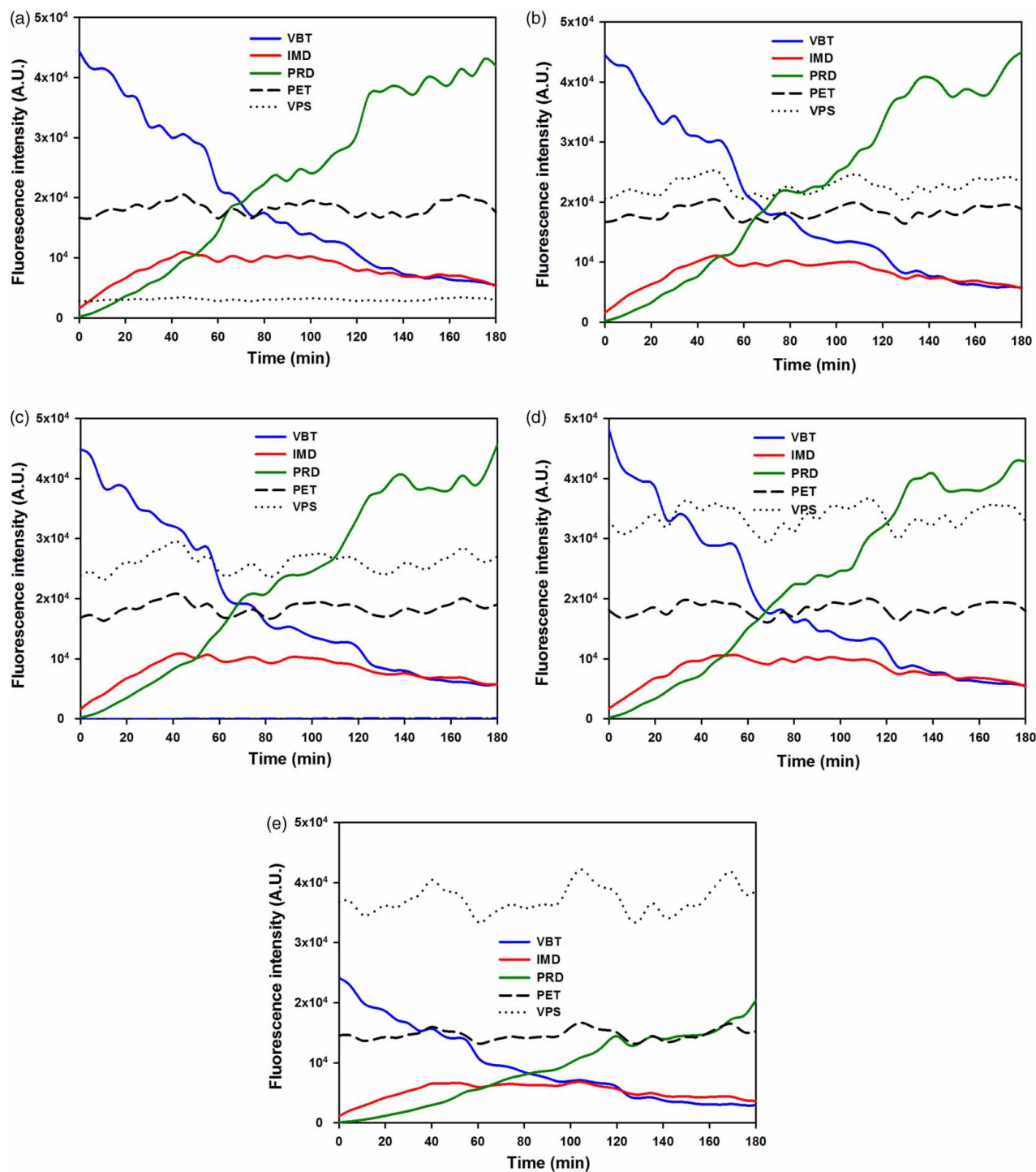
Figure 5. MCR-ALS kinetics profiles for five different VBT:VPS$_m$ copolymer ratios: (a) VBT:VPS$_1$; (b) VBT:VPS$_4$; (c) VBT:VPS$_8$; (d) VBT:VPS$_{16}$ and (e) VBT:VPS$_{32}$.

(IMD) increases. At longer irradiation times, as the intermediate species is consumed, a growth of the final product (PRD) signal is observed. Making use of these results and Equation (2) (Section 2), it is possible to identify the kinetics profiles of the species

involved in the curing reaction (Figure 5). Interestingly, the kinetics profiles are in agreement with reported results for VBT-VBA copolymers (*16, 18*), suggesting that the curing process is only VBT-dependent. On the other hand, for each copolymer

composition, the VPS species remains constant throughout the entire cross-linking reaction, while as the concentration of the VPS interferent augments, the chemometric resolution gets worse (Figure 5(e)). Furthermore, the PET spectrum overlaps with the relevant signals being an important factor to explain the fair performance of the algorithm. Consequently, the quantitative resolution deteriorates.

Regarding the information obtained about the copolymers kinetics, unfortunately the initial concentration of the reactants cannot be unmistakably identified since the samples were processed individually. This fact represents a major disadvantage of the strategy used, providing the results cannot be used to characterize similar samples of uncertain origin. Meanwhile, the kinetic constants of the process cannot be calculated because the proposed species which are actually involved in the process cannot be accurately established, as described below.

Even though in general, the resolved emission spectra of the different copolymer compositions analyzed are similar, it is also true that there are noticeable differences establishing uncertainties to the conclusions reached (see Figure 4(b)–(d)). The strong PET signal (representing around 20% of the measured signal for VBT:VPS$_1$ while for VBT:VPS$_{32}$ reaches 50%, see Figure 4(a)–(c)) and the extreme overlapping of all species in the emission (Figure 4(b)–(d)) and excitation mode (indirectly observed in Figure 4(a)–(c)) cause the deficiency of the three-way model to provide suitable responses. Indeed, Table 1 presents the selectivities found by the three-way MCR-ALS model, in contrast with the four-way MCR-ALS model (discussed below). All computed values are poorer for the three-way model than for the four-way model.

In order to improve the outcomes, a super-augmented **D** matrix including all samples was built by appending the third-order data matrices (irradiation time-unfolded EEFMs). The non-negativity constraint for all concentration sub-profiles was applied during the ALS optimization to get physical meaningful

Table 1. Selectivities calculated according to Equation (3) by the three- and four-way MCR-ALS models.

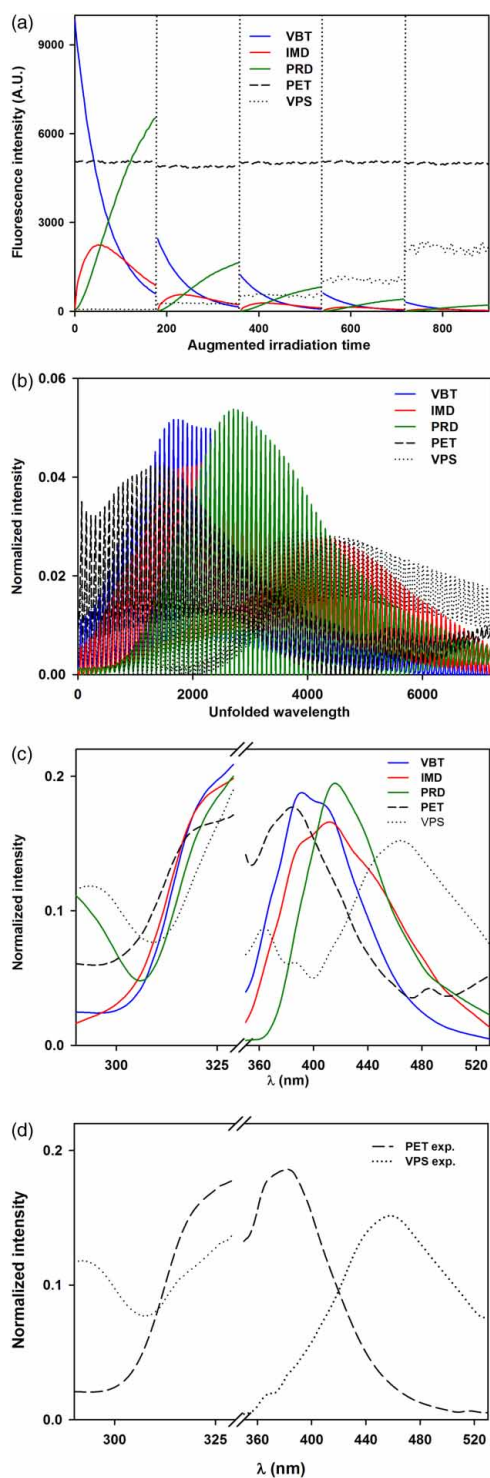|	VBT	Intermediate	Product	PET	VPS
Three-way					
VBT:VPS$_1$	0.21	0.22	0.30	0.63	0.54
VBT:VPS$_4$	0.17	0.24	0.24	0.67	0.41
VBT:VPS$_8$	0.17	0.21	0.25	0.57	0.38
VBT:VPS$_{16}$	0.15	0.23	0.23	0.53	0.63
VBT:VPS$_{32}$	0.12	0.23	0.25	0.48	0.38
Four-way	0.40	0.50	0.36	0.66	0.61

Figure 6. Profiles obtained by the four-ways MCR-ALS method. (a) Augmented time profiles for each species, where dotted bars indicate the end of each sub-profile, (b) unfolded EEFM profiles for each species, (c) refold of unfolded EEFM profiles to obtain the excitation and emission profiles for each species (see text) and (d) experimental excitation and emission spectra for PET (λ_{exc} = 320 nm, λ_{ems} = 380 nm) and aqueous VPS solution 10% w/w (λ_{exc} = 295 nm, λ_{ems} = 450 nm).

solutions. The number of compounds (five, as in the second-order analysis) and the initial spectra were supplied similarly to the three-way analysis. After MCR-ALS decomposition of **D** according to Equation (1), the concentration information contained in **C** was used to assemble the pseudo-univariate graph by plotting the analyte concentration scores against the nominal analyte concentrations (Equation (2)).

Figure 6 shows the profiles resolved by the four-ways MCR-ALS method for the sample set. Figure 6 (a) presents the augmented irradiation time profiles and Figure 6(b) the unfolded EEFM profiles for each species, while Figure 6(c) shows the emission and excitation profiles of all compounds in the sample set obtained via refold of the S^T matrix (Equation (1)). This refold was made by creating a suitable data matrix, submitted to singular value decomposition, and taking the first left and right eigenvectors as estimations of the true component profiles in both data modes. This process is essential to determine that the information achieved by the algorithm is in good agreement with the experimental data. Comparing the spectra with data reported in refs. (22–24), as well as with the spectra obtained experimentally for PET and VPS (Figure 6(d)), a reasonable agreement was observed; in fact, the correlation between experimental and modeled spectra was evaluated in terms of similarity coefficients (26), obtaining values of 0.953 and 0.949 for PET emission and excitation spectra, and 0.998 and 0.979 for VPS emission and excitation spectra, respectively. Regarding the spectral features of the excitation and emission profiles assigned to VBT (blue line in Figure 6(c)), reported data for

thymine fluorescence (20) indicate a comparable emission maximum at 400 nm ($\lambda_{exc} = 295$ nm), even if no quantitative evaluation of such similarity is possible. Finally, the refolded spectral profiles designed for the species generated in the curing reaction are in agreement with previously reported data (16, 18), allowing us to make a suggestion of the species involved in the curing process (see Scheme 1).

On the other hand, the refolded spectral profiles obtained for the five species involved in the curing process are similar to the spectra resolved in the three-way MCR-ALS analysis (Figure 4(b)–(d)). Nevertheless, in the four-way method, the unfolded spectra are significantly less ambiguous than those in the three-way approach, since each species has a single pair of excitation-emission spectra irrespective of the copolymer composition tested. These characteristics are consistent with the selectivities achieved by the third-order algorithm for the compounds, as clearly seen for all cases in Table 1.

Concerning the irradiation time profiles, it is important to note that each profile is the combination of all copolymer compositions, and therefore the profiles should be sorted according to Equation (2) to predict the concentration of the compounds of interest in each sample of the set. Figure 6(a) shows the kinetics of the curing reaction as a function of irradiation time and the percentage of VBT in the copolymer sample. The kinetic curves match for the most part those reported in the literature for similar copolymers (16, 18). In addition they show a substantial improvement compared to the curves achieved with the second-order analysis (Figure 5).
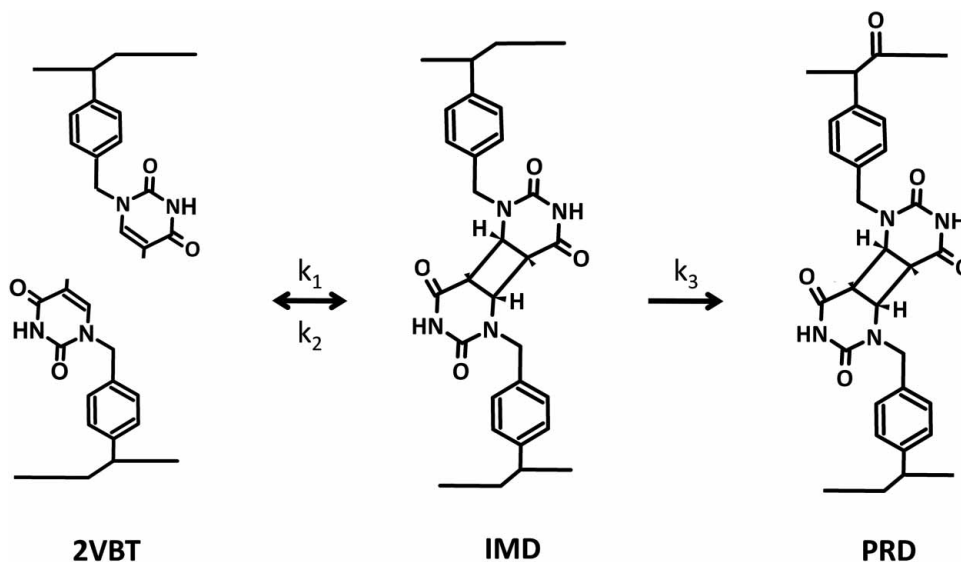
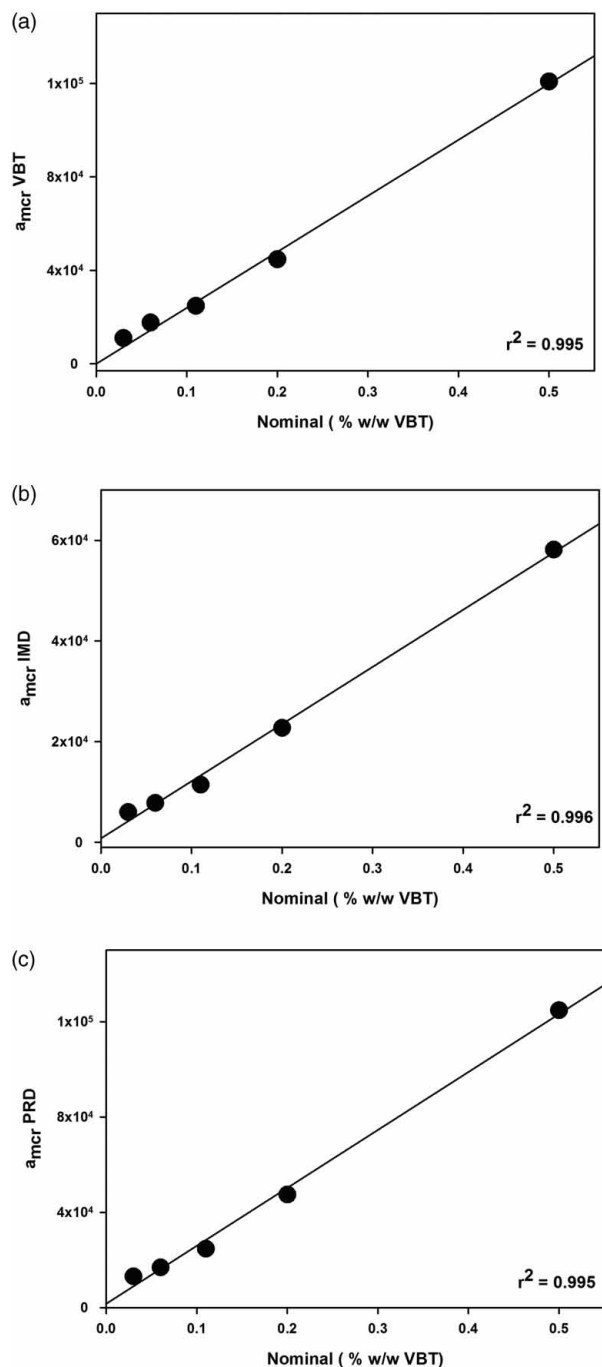Scheme 1. Proposed structures for the species involved in VBT-VPS curing process.

Figure 7. Regression curves for the three meaningful species, according to third-order chemometric approach. In all cases, the curves correlate the MCR scores (see Equation (2)) with the nominal concentrations of VBT in the different samples; the r^2 coefficients are shown in each case. (a) VBT, (b) IMD and (c) PRD.

In Bortolato et al., (*16, 18*) a characterization of the cross-linking process evolution for VBT copolymers was accomplished using a chemometric algorithm, and a VBT-dependent kinetic mechanism was proposed as follows:

$$2\text{VBT} \underset{k2}{\overset{k1}{\longleftrightarrow}} \text{IMD} \overset{k3}{\longrightarrow} \text{PRD}$$

being the reaction rates:

$$dy_{\text{VBT}}/dt = -k_1 y^2{}_{\text{VBT}} + k_2 y_{\text{IMD}},$$

$$dy_{\text{IMD}}/dt = k_1 y^2{}_{\text{VBT}} - k_2 y_{\text{IMD}} - k_3 y_{\text{PRD}}, \quad (4)$$

$$dy_{\text{PRD}}/dt = k_3 y_{\text{IMD}}.$$

Numerically solving the ordinary differential equations (Equation (4)) and using the experimental concentration values as well as a set of trial rate constants as inputs, the kinetic evolutions can be obtained (*34*).

Using the same kinetic scheme and comparing the kinetic evolutions with the experimental data for all VBT-VPS copolymers, the following rate constants were found: $k_1 = 1250$ $\text{M}^{-1}\text{s}^{-1}$, $k_2 = 2$ $\text{M}^{-1}\text{s}^{-1}$ and $k_3 = 4$ $\text{M}^{-1}\text{s}^{-1}$. The ratios between the constants are in agreement with previously reported kinetic rate values for VBT-VBA copolymers, which reinforces the assumption that the kinetic mechanism is VBT-dependent (*18*). Additionally, the predicted MCR-ALS spectra and kinetic profiles for five VBT:VPS copolymer ratios presented in Figure 6 may well be used to build a regression model, considering the VBT content of the reaction system: VBT:VPS$_1$ (50% w/w VBT), VBT:VPS$_4$ (20% w/w VBT), VBT:VPS$_8$ (11% w/w VBT), VBT:VPS$_{16}$ (6% w/w VBT) and VBT:VPS$_{32}$ (3% w/w VBT). The results of such regression model are shown in Figure 7. A good correlation between the MCR scores and the nominal concentration of VBT can be seen for the three meaningful species (VBT, IMD and PRD), indicating that the chemometric resolution is satisfactory, regardless of the presence of two interferents (VPS and PET). In this case, it was possible to make use of the second-order advantage despite having a more complicated system. Besides, this outcome allows affirming without any doubt that the curing reaction is VBT-dependent and is second order with respect thereto, with constant values similar to the previously reported rates (*18*).

5. Conclusions

The photo-induced curing kinetics of bioinspired copolymers VBT and VPS was studied using fluorescence spectroscopy in combination with multivariate chemometric algorithms. The emission and excitation fluorescence spectra were recorded for different

copolymer compositions and irradiation doses, and their effect was analyzed without the need of sample pre-treatments.

Two chemometric strategies were used to decompose the data matrix generated while monitoring the cross-linking reaction, identifying the evolution of each species involved in the process in conjunction with the corresponding pure spectra. A complete comparison between the developed chemometric approaches was performed, clearly highlighting the advantages and disadvantages of both.

It was found that the evolution of the curing process of the VBT-VPS copolymers involved three species clearly present in the reaction, plus two species interfering on the measured signal but not influenced by the irradiation time. The determination of the number of species involved in the curing reaction is significant to establish the necessary conditions to produce cross-linked polymers. The contribution of each species to the total signal at each irradiation time was anticipated, which enabled to estimate the kinetic constant of the process as a function of VBT content.

In summary, it was possible to use two analytical approaches that combine solid-phase fluorescence and chemometric tools to provide accurate information on the photo-induced VBT-VPS copolymer immobilization, together with the kinetics of all the species involved. This information is essential for developing new environmentally benign materials with pre-specified quality and properties.

The choice of this analytic strategy is not trivial. It would be possible to propose a separative scheme that involves selective reagent and/or product removal from the PET substrate and chromatographic quantification of the species along the reaction time. On the other hand, the use of solid-phase fluorescence cannot assure, on its own, the answer to the problem. It is necessary to add the chemometric step in order to identify the relevant signals and the non-reactive species.

In this way, we conquer a greener analytical approach to solve the problem, which is based on direct measurements of untreated samples, no sophisticated equipment is required, analysis time is reduced and the use of toxic solvents is avoided.

Acknowledgments

Disclosure statement

Funding

References

(1) (a) Blackburn, G.M.; Davies, R.J.H. *J. Chem. Soc. C.* **1966**, 2239; (b) Lamola, A.A.; Mittal, J.P. *Science* **1966**, *154*, 1560.

(2) Cheng, C.; Egbe, M.; Grasshoff, J.; Guarrera, D.; Pai, R.; Warner, J.; Taylor, L. *J. Polym. Sci. Polym. Chem.* **1995**, *33*, 2515–2519.

(3) Trakhtenberg, S.; Hangun-Balkir, Y.; Warner, J.; Bruno, F.; Kumar, J.; Nagarajan, R.; Samuelson, L. *J. Am. Chem. Soc.* **2005**, *127*, 9100–9104.

(4) Kiarie, C.; Bianchini, J.; Trakhtenberg, S.; Warner, J.C. *J. Macromol. Sci. Part A Pure and Appl. Chem.* **2005**, *42*, 1489–1496.

(5) Casis, N.; Luciani, C.V.; VichBerlanga, J.; Estenoz, D.A.; Martino, D.M.; Meira, G.R. *Green Chem. Lett. Rev.* **2007**, *1*, 65–72.

(6) Whitfield, J.; Morelli, A.; Warner, J.C.; *J. Macromol. Sci. Part A Pure Appl. Chem.* **2005**, *42*, 1541–1546.

(7) Grasshoff, J.; Taylor, L.; Warner, J. U.S. Patent 5 395 731 **1995**.

(8) Grasshoff, J.; Taylor, L.; Warner, J. U.S. Patent 5 455 349 **1995**.

(9) Grasshoff, J.; Taylor, L.; Warner, J. U.S. Patent 5 616 451 **1997**.

(10) Grasshoff, J.; Taylor, L.; Warner, J. U.S. Patent 5 708 106 **1998**.

(11) Barbarini, A.; Martino, D.M.; Estenoz, D. *Macromolecular Reaction Eng.* **2010**, *4*, 453–459.

(12) Olivieri, A. *Anal. Chem.* **2008**, *80*, 5713–5720.

(13) Armenta, S.; Garrigues, S.; de la Guardia, M. *Trends Anal. Chem.* **2008**, *27*, 497–511.

(14) Jaumot, J.; Gargallo, R.; de Juan, A.; Tauler, R. *Chemometr. Intell. Lab.* **2005**, *76*, 101–110.

(15) Garrido, M.; Rius, F.X.; Larrechi, M.S. *Anal Bioanal Chem.* **2008**, *390*, 2059–2066.

(16) Bortolato, S.A.; Thomas, K.E.; McDonough, K.; Gurney, R.W.; Martino, D.M. *Polymer.* **2012**, *53*, 5285–5294.

(17) Faber, N.M.; Ferre, J.; Boque, R.; Kalivas, J.H. *Trends Anal. Chem.* **2003**, *22*, 352–361.

(18) Bortolato, S.A.; McDonough, K.; Gurney, R.W.; Martino, D.M. *Talanta.* **2014**, *127*, 204–210.

(19) Galuszka, A.; Migaszewski, Z.; Namiesnik, J. *Trends Anal. Chem.* **2013**, *50*, 78–84.

(20) Morsy, M.A.; Al-Somali, A.M.; Suwaiyan, A. *J. Phys. Chem. B*. **1999**, *103*, 11205–11210.

(21) Ledesma, J.; Bortolato, S.A.; Boschetti, C.E.; Martino, D.M. *J. Chem*. **2013**, Article ID 947137, 9 pages http://dx.doi.org/10.1155/2013/947137.

(22) Sonnenschein, M.F.; Roland, C.M. *Polymer*. **1990**, *31*, 2023–2026.

(23) Ouchi, I.; Miyamura, R.; Sakaguchi, M.; Hosaka, S.; Kitagawa, M. *Polym. Ad. Technol*. **1999**, *10*, 195–198.

(24) Itagaki, H.; Arakawa, S. *Polymer*. **2009**, *50*, 1491–1496.

(25) Jaumot, J.; Vives, M.; Gargallo, R.; Tauler, R. *Anal. Chim. Acta*. **2003**, *490*, 253–264.

(26) De Juan, A.; Casassas, E.; Tauler, R. In *Encyclopedia of Analytical Chemistry*: Meyers, R.A., Ed.; John Wiley & Sons: Chichester, **2000**; p. 9800.

(27) Parastar, H.; Radović, J.R.; Jalali-Heravi, M.; Diez, S.; Bayona, J.M.; Tauler, R. *Anal. Chem*. **2011**, *83*, 9289–9297.

(28) Alcaráz, M.R.; Siano, G.; Culzoni, M.J.; Muñoz de la Peña, A.; Goicoechea, H.C. *Anal. Chim. Acta*. **2014**, *809*, 37–46.

(29) Escandar, G.M.; Goicoechea, H.C.; Muñoz de la Peña, A.; Olivieri, A.C. *Anal. Chim. Acta*. **2014**, *806*, 8–26.

(30) Windig, W.; Guilment, J. *Anal. Chem*. **1991**, *63*, 1425–1432.

(31) Bauza, M.C.; Ibañez, G.A.; Tauler, R.; Olivieri, A.C. *Anal. Chem*. **2012**, *84*, 8697–8706.

(32) MacLeod, D.M. In *Coatings Technology Handbook*, 2nd ed.; Satas, D., Tracton, A.A., Eds.; Marcel Dekker: New York, **2001**; pp 129–138.

(33) *MATLAB 7.0*, The Mathworks: Natick, MA, **2007**.

(34) *MATHEMATICA 7.0*, Wolfram Research: Champaign, IL, **2009**.